



**HAL**  
open science

## Quenched polyelectrolytes with hydrophobicity independent from chemical charge fraction: A SANS and SAXS study

Souha Ben Mahmoud, Wafa Essafi, Amira Abidelli, Michel Rawiso, François Boue

► **To cite this version:**

Souha Ben Mahmoud, Wafa Essafi, Amira Abidelli, Michel Rawiso, François Boue. Quenched polyelectrolytes with hydrophobicity independent from chemical charge fraction: A SANS and SAXS study. *Arabian Journal of Chemistry*, 2017, 10 (7), pp.1001-1014. 10.1016/j.arabjc.2017.02.003 . hal-02626372

**HAL Id: hal-02626372**

<https://hal.inrae.fr/hal-02626372>

Submitted on 26 May 2020

**HAL** is a multi-disciplinary open access archive for the deposit and dissemination of scientific research documents, whether they are published or not. The documents may come from teaching and research institutions in France or abroad, or from public or private research centers.

L'archive ouverte pluridisciplinaire **HAL**, est destinée au dépôt et à la diffusion de documents scientifiques de niveau recherche, publiés ou non, émanant des établissements d'enseignement et de recherche français ou étrangers, des laboratoires publics ou privés.



Distributed under a Creative Commons Attribution - NonCommercial - NoDerivatives 4.0 International License



ORIGINAL ARTICLE

# Quenched polyelectrolytes with hydrophobicity independent from chemical charge fraction: A SANS and SAXS study



Souha Ben Mahmoud<sup>a,b</sup>, Wafa Essafi<sup>a,\*</sup>, Amira Abidelli<sup>a</sup>, Michel Rawiso<sup>c</sup>, François Boué<sup>d,e</sup>

<sup>a</sup> *Laboratoire Matériaux, Traitement et Analyse, Institut National de Recherche et d'Analyse Physico-Chimique, Pôle Technologique de Sidi Thabet, 2020 Sidi Thabet, Tunisia*

<sup>b</sup> *Institut National des Sciences Appliquées et de Technologie, Centre Urbain Nord BP 676, 1080 Tunis Cedex, Tunisia*

<sup>c</sup> *Institut Charles Sadron (UPR22 CNRS-UdS), 23 rue du Loess - BP 84047, 67034 Strasbourg Cedex 2, France*

<sup>d</sup> *Génie et Microbiologie des Procédés Alimentaires, UMR782 INRA-AgroParisTech, 1 Avenue Lucien Brétignières, 78850 Thiverval, Grignon, France*

<sup>e</sup> *Laboratoire Léon Brillouin (UMR12 CNRS-IRAMIS-CEA), CEA Saclay Bât 563, 91191 Gif-sur-Yvette Cedex, France*

Received 18 October 2016; accepted 11 February 2017

Available online 28 February 2017

## KEYWORDS

Polyelectrolyte solution;  
Hydrophobic;  
SAXS;  
SANS;  
Collapsed;  
Conformation;  
Pearl necklace

**Abstract** We investigate by SANS and SAXS the structure of semidilute aqueous hydrophobic quenched polyelectrolyte solutions, in which we can vary independently the hydrophobicity and the chemical/electrostatic charge fraction (above the Manning condensation threshold 36%). Such a de-correlation is the original point of the work, reached using statistical tri-copolymers poly(acrylamide-co-styrene-co-2-acrylamido-2-methylpropane-sodium sulfonate), poly(AM<sub>x</sub>-co-ST<sub>y</sub>-co-AMPS<sub>z</sub>). The hydrophobicity is brought by ST, the chemical electrostatic charge by AMPS and solubility without charge by AM. We consider that although these copolymers have chemical structure different from partially sulfonated polystyrene sulfonate, PS-co-SSNa, made of two monomers, one charged, one hydrophobic, they have however vicinal behavior. The variation of chemical charge, has no strong consequence on the structure properties which is in agreement with the fact that it is always larger than the Manning threshold. The dependence of  $q^*$  with AM content shows that AM reduces hydrophobicity. The similarity with PS-co-SSNa, for which pearl necklace-like conformations were directly measured by SANS (form factor using ZAC method), suggests that pearl necklace conformations are also adopted by these tri-copolymers and that this behavior could

\* Corresponding author.

E-mail addresses: wafa.essafi@wanadoo.fr, essafi.wafa@inrap.rnrt.tn (W. Essafi).

Peer review under responsibility of King Saud University.



be so generalized to a much larger range of synthetic hydrophobic polyelectrolytes using simple copolymerization.

© 2017 The Authors. Production and hosting by Elsevier B.V. on behalf of King Saud University. This is an open access article under the CC BY-NC-ND license (<http://creativecommons.org/licenses/by-nc-nd/4.0/>).

## 1. Introduction

Polyelectrolytes (PE) form a very important class of water soluble polymers; they may contain a variable proportion of ionizable monomers. In polar solvent with a high dielectric constant, the charges of one sign are localized on the chain whereas the counterions, of opposite sign, are distributed in the whole solution. The behavior of the polyelectrolytes in the solution and their chain conformation are monitored by the degree of hydrophobicity, and the electrostatic interactions, i.e. the effective charge fraction (which depends on the chemical charge fraction, and the hydrophobic interactions). Hydrophilic polyelectrolytes are under good solvent conditions in water, and the interactions have a pure electrostatic nature. For hydrophobic PE, the balance hydrophobic/hydrophilic is high and must be taken into account.

Let us recall the general background about polyelectrolytes chain conformation and interactions in solvent, say water. We start by the dilute regime. For the hydrophilic polyelectrolytes, the single chain is theoretically described as an extended rod-like configuration of electrostatic blobs (de Gennes et al., 1976; Dobrynin et al., 1995; Barrat et al., 1996). For hydrophobic polyelectrolytes, the pearl-necklace model (Dobrynin et al., 1996; Rayleigh, 1882; Dobrynin and Rubinstein, 1999; Dobrynin and Rubinstein, 2001) has been the most elegant one proposed (Scheme 1a). The balance between collapse and extension results in the formation of compact beads (the pearls) of diameter  $D_{\text{pearl}}$  joined by elongated strings of thermal blobs of size  $\xi_T \ll D_{\text{pearl}}$ , in agreement with simulations (Micka et al., 1999; Limbach et al., 2002; Limbach and Holm, 2003; Schweins and Huber, 2004; Liao et al., 2006).

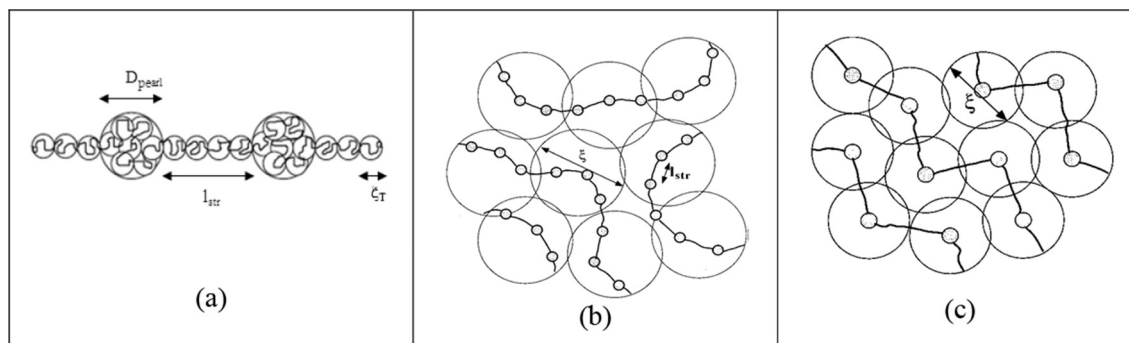
In the semidilute regime, the concentration  $c_p$  is larger than a threshold  $c_p^*$ , above which the volume occupied by each chain overlaps the one occupied by the neighbor chains. The highly charged polyelectrolytes in good solvent are theoretically described by the isotropic model, in which the chains are interpenetrated and form an isotropic transient network of mesh  $\xi$  (de Gennes et al., 1976; Dobrynin et al., 1995).

The polyelectrolyte chain is still a random walk of correlation blobs of size  $\xi$ , each one being an extended configuration of electrostatic blobs of size  $\xi_{\text{el}}$ . In the case of hydrophilic polyelectrolyte,  $\xi$  scales with polyelectrolyte concentration as  $c_p^{-1/2}$ , (de Gennes et al., 1976; Dobrynin et al., 1995) as early verified by SANS (Nierlich et al., 1979, 1985; Jannink, 1986) and SAXS for high chemical charge fractions  $f_{\text{chem}}$  (Essafi et al., 1999). There is also a predicted scaling of  $\xi$  with the actual charge fraction  $f_{\text{chem}}$ , including the case where  $f_{\text{chem}}$  is reduced by Oosawa-Manning (Oosawa, 1971; Manning, 1969) counterion condensation (Combet et al., 2005, 2011). In the case of hydrophobic polyelectrolyte, two regimes are predicted by Dobrynin and Rubinstein (1999, 2001): the string controlled regime, similar to the one observed in the hydrophilic case ( $\xi \sim c_p^{-1/2}$ ,  $\xi > l_{\text{str}}$ , the string length between two neighboring beads, see Scheme 1b), and the bead-controlled regime  $\xi \sim c_p^{-1/3}$  (Dobrynin and Rubinstein, 1999, 2001) where the system behaves as a solution of charged beads of constant size (see Scheme 1c).

Let us then describe the experimental situation, especially when scattering measurements are used, like in our previous paper on the subject (Essafi et al., 2011). The latter is part of a series addressing the pearl necklace model using partially sulfonated polystyrene (polystyrene-co-styrene sodium sulfonate, PS-co-SSNa). The corresponding chain chemical structure is slightly different from the theoretical situation since it is a random copolymer of two different segments, ionizable hydrophilic ones (sulfonated) and hydrophobic ones (not sulfonated).

In most of the cases these experimental results relied on scattering experiments. It was first shown by SAXS some years ago that the polyelectrolyte chains, which were initially worm-like, had collapsed into more compact objects, as the hydrophobicity increases. Subsequently, the objects become further from each other (Williams et al., 2001; Baigl et al., 2003a,b; Essafi et al., 1994).

Another group, using addition to water of acetone (a bad solvent, or marginal solvent), showed that poly(methacryloyle thyltrimethyl ammonium methyl sulfate) underwent a coil to globule collapse transition (Aseyev et al., 1998, 2001). A third



**Scheme 1** Pearl necklace model for hydrophobic polyelectrolyte in dilute regime (a), semidilute string controlled regime (b), and semidilute bead-controlled regime (c). Reprint with authorization from paper of Dobrynin and Rubinstein (1999).

system dealt with specifically interacting alkaline earth cations which can neutralize anionic chains (Schweins et al., 2003; Goerigk et al., 2004).

Experimentally the most interesting scattering results have been found in the semidilute regime. In most of the cases, the scattered intensity measured by SAXS or SANS, was corresponding to the total structure function  $S_T(q)$ , which, when all chains have the same contrast with the solvent, comes mostly from pairs of scatterers coming from two different chains.  $S_T(q)$  displays a maximum at  $q^* = 2\pi/\xi$ . It was found for PSSNa that  $\xi$  scales as  $c_p^{-\alpha < 0.4}$  when the chemical charge fraction  $f_{chem}$  decreases (Essafi et al., 1994; Spiteri, 1997; Spiteri et al., 2007). This behavior was also seen when associating SAXS and atomic force microscopy studies (Baigl et al., 2003a,b; Dan Qu et al., 2003). Apart from scattering, the evidence for low internal dielectric constant  $\epsilon$  (Essafi et al., 1995) regions and the reduction in osmotic pressure (Essafi et al., 2005) - hence of effective charge, were observed. In other words the counterion condensation was shown larger for compacted chain than for the hydrophilic case where Manning-Oosawa (Oosawa, 1971; Manning, 1969) law applied. A theoretical derivation was given later (Chepelianskii et al., 2009).

Last but not least, the average conformation of the polystyrene-co-styrene sodium sulfonate chain was addressed, mostly in semidilute regime using the SANS - Zero Average Contrast (ZAC) method (Spiteri, 1997; Spiteri et al., 2007), a fraction of PS-co-SSNa chains being deuterated. The existence of compact regions was unambiguously observed, and the form factor could be described by the pearl necklace model, in partial agreement with Schweins and Huber (2004) and full agreement with Liao et al. (2006).

Hence a quasi-complete description could be achieved for partially sulfonated polystyrene. **However, let us recall that this polymer is slightly different of the ideal picture for pearl necklace.** Instead of being partly hydrophobic on each unit, it is a copolymer of ionizable segments (sulfonated) and hydrophobic segments (not sulfonated), i.e. poly(sodium styrene sulfonate) $_{f_{chem}}$ -styrene $_{1-f_{chem}}$ . A first possible consequence of this copolymer structure is the existence of long sequences (which would artificially create pearls), which however have never been detected. A second consequence of such copolymer structure is that, when the chemical charge fraction  $f_{chem}$  is varied, the content of hydrophobic segments is varied too: the two features could not be varied independently.

In order to improve these two aspects, we propose the following:

- to use a type of synthesis different from partial sulfonation of a polymer. One can imagine that a well conducted copolymerization may produce sequences of the same monomer (AM, ST or AMPS) with differently distributed length (e.g. more statistically) than for sulfonation.
- to vary independently the chemical charge fraction  $f_{chem}$  and the hydrophobic segment fraction, i.e. if we change the hydrophobic content, we can keep constant the chemical ionizable segment charge fraction  $f_{chem}$  and vice versa (we keep in mind that the final effective charge  $f_{eff}$  depends on the degree of counterion condensation).

For that purpose, we will use copolymerization of different monomers as a synthesis approach, and will start from three different monomers. We will use one hydrophilic neutral

monomer (acrylamide), a second hydrophobic neutral monomer (styrene) and a third charged hydrophilic monomer (sodium-2-acrylamido-2-methylpropane sulfonate). They will be copolymerized in a “tri-co-polyelectrolyte”. The chemical charge fraction, will then be given by the fraction of charged hydrophilic monomer, while the hydrophobicity will be determined by the fraction of the hydrophobic neutral monomer and of the neutral hydrophilic one.

Note that Di Cola et al. (2004) considered already di-copolymers resulting from copolymerization: sodium maleate copolymerized with isobutylene (IBMA), diisobutylene (DIBMA), styrene (SMA), on the one hand, and with *d* 1-alkenes with *m*) 8, 10, 12, 14 carbons (*n*-CmMA), on the second hand. SANS and SAXS data were consistent with a distinct demarcation between the so-called hydrophobically modified polyelectrolytes (HMPE) behavior,  $q^* \sim c_p^{1/3}$ , from complete collapsed chains, and “mildly hydrophobic” copolymers, for which  $q^* \sim c_p^{1/2}$  in average, which was discussed in the frame of the string dominated Dobrynin Rubinstein (DR) model. This point of view is different from the detailed monitoring of  $q^*$  with the hydrophobicity which we will propose in the present paper, and the polyelectrolytes were bicopolymers, not tri-copolymers like we propose.

In summary, the aim of the present work was to investigate the structure of those aqueous “tri-co-polyelectrolyte” solutions, to modulate the hydrophobicity of the polyelectrolyte while keeping unchanged the chemical charge fraction, or the reverse. We do this by using Small Angle Neutron and X-ray Scattering in the semidilute regime to determine the total structure function  $S_T(q)$  (the study of chain conformation is not possible without deuteration). We wish to differentiate between the role of the rate of hydrophobicity and the rate of electrostatic/chemical charge on the polyelectrolyte solution structure.

## 2. Experimental

### 2.1. Polymer synthesis

The tri-co-polyelectrolyte noted (AMx-STy-AMPSz), the chemical structure of which is shown in Fig. 1, is a random copolymer made out of three monomers: acrylamide whose rate is  $x/(x + y + z)$ , styrene whose rate is  $y/(x + y + z)$  and 2-Acrylamido-2-methyl-1-propane sulfonic acid sodium salt whose rate is  $z/(x + y + z)$ . This polyelectrolyte is characterized by decorrelated electrostatic charge and hydrophobic fractions, i.e. the hydrophobicity rate “ $y/x + y + z$ ” can be varied, within a certain range, without changing the electrostatic charge fraction “ $z/x + y + z$ ” and vice versa.

Acrylamide, styrene and N,N dimethylformamide (DMF) were purchased from Sigma Aldrich, the 2-acrylamido-2-methylpropane sulfonic acid and the benzoyl peroxide were

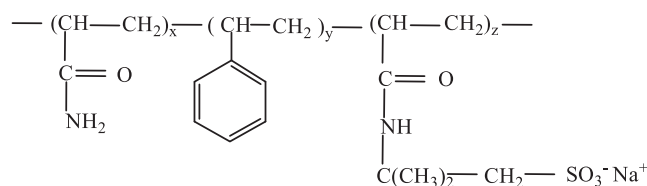


**Figure 1** Chemical Structure of poly(AMx-STy-AMPSz), the chemical charge fraction is  $f_{chem} = z/x + y + z$ .

**Table 1** Monomer feed ratios and tri-co-polyelectrolyte composition.

Monomer feed ratio %			Tri-co-polyelectrolyte composition	Conversion %
AM(x)	ST(y)	AMPS(z)		
10	40	40	AM17-ST17-AMPS66	58
5	40	40	AM26-ST23-AMPS51	53
2	80	40	AM05-ST67-AMPS28	37
20	10	60	AM40-ST04-AMPS56	62
5	55	60	AM17-ST44-AMPS39	41
10	20	70	AM23-ST06-AMPS71	58
10	50	40	AM20-ST55-AMPS25	42
3	52	45	AM10-ST50-AMPS40	40

purchased from Scharlau and sodium hydroxide was from Carlo Erba. All the reagents were used as received.

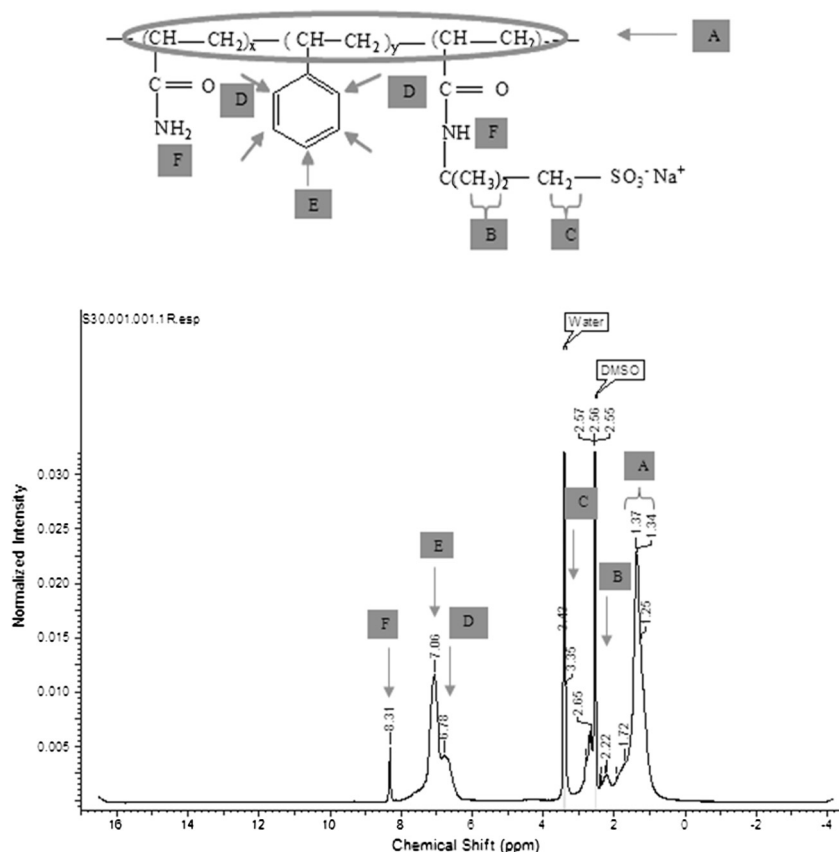
The poly(AM<sub>x</sub>-ST<sub>y</sub>-AMPS<sub>z</sub>) was prepared by direct polymerization of the three monomers with a free-radical initiator in the N,N dimethylformamide or cyclohexane in case of high styrene content ( $y > 40\%$ ). This method is inspired from that of Peiffer et al. (1988) used to prepare copolymers of styrene and 2-acrylamido-2-methylpropane sodium sulfonate.

The experimental data of the resulting tri-co-polyelectrolyte are summarized in Table 1. An example of a polymerization of the tri-co-polyelectrolyte AM26-ST23-AMPS51, is described as follows. A three-necked 100 ml contains a solution of AMPS (7.45 g) in DMF 12 ml, then a solution of acrylamide (0.42 g in 1 ml DMF) was added to the mixture and finally styrene (2.4 ml) was added. The mixture was stirred for

approximately 2 h under nitrogen gas at room temperature. The used initiator, benzoyl peroxide, was subsequently added (0.11 g in 1 ml DMF) and the solution temperature adjusted to 70 °C. The temperature was controlled continually throughout the polymerization time depending on the chemical charge (i.e. 4–12 h). Also, the solution was stirred continually during the reaction and kept flooded with dried nitrogen.

Depending on the polymer composition, the tri-co-polyelectrolyte precipitation occurred during the polymerization when the % of styrene is low ( $< 40\%$ ), which rendered it easy to recover. But when styrene % was high, the polymer remained in cyclohexane solution; in this case it had to be recovered by precipitation in ethanol.

The resulting tri-copolymer was then dissolved in aqueous solution and neutralized with sodium hydroxide, purified by dialysis, concentrated and freeze dried.

**Figure 2** <sup>1</sup>H NMR of AM17-ST44-AMPS39 in DMSO-*d*<sub>6</sub>.

## 2.2. Polymer chemical characterization

### 2.2.1. NMR

The  $^1\text{H}$  NMR,  $^{13}\text{C}$  NMR spectroscopies and Elemental Analysis were used to determine the chemical composition of the synthesized tri-co-polyelectrolyte.

The NMR measurements were made using Ultra shield 500 plus at the Institut National de Recherche et d'Analyse Physico-Chimique (INRAP)-Sidi Thabet. The frequency is equal to 500 MHz for  $^1\text{H}$  NMR and 125 MHz for  $^{13}\text{C}$  NMR. Two solvents were used for NMR analysis:  $\text{D}_2\text{O}$  for hydrophilic polyelectrolyte and  $\text{DMSO-}d_6$  for hydrophobic polyelectrolyte.

The NMR was mainly used to check the presence of the three monomers on the resulting polyelectrolyte but cannot be quantitative due to the overlapping of some resonance peaks.

Fig. 2 shows a typical  $^1\text{H}$  NMR spectrum of a tri-co-polyelectrolyte in  $\text{DMSO-}d_6$ . It is composed of a broad band ( $\delta = 1.25\text{--}1.55$  ppm) corresponding to the aliphatic protons of the polymer backbone (that of styrene, acrylamide and 2-acrylamido-2-methylpropane sodium sulfonate). The protons of  $\text{CH}_3$  groups in AMPS are detected at around 2.0 ppm and the signal of the  $\text{CH}_2$  group bonded to  $\text{SO}_3\text{Na}$  is detected at 3.2 ppm (Jamshidi and Rabiee, 2014).

The sharp peak at  $\delta = 2.56$  ppm corresponds to the residual protons from the imperfect deuteration of the solvent  $\text{DMSO}$  and the second one at  $\delta = 3.42$  ppm is attributed to water either in the solvent or as the residual water in the polyelectrolyte powder (Baigl et al., 2002). The signals at  $6\text{ ppm} < \delta < 7\text{ ppm}$  correspond to the presence of the aromatic zone hydrogen of the styrene monomer. Finally, the peak at  $\delta = 8.31$  ppm corresponds to the protons of the amide function of acrylamide and 2-acrylamido-2-methylpropane sodium sulfonate.

In the  $^{13}\text{C}$  NMR spectrum of the same tri-co-polyelectrolyte of AM17-ST44-AMPS39 in  $\text{DMSO-}d_6$ , the presence of  $\text{C} = \text{O}$  function in AM and AMPS gives a peak around 176.6 ppm (Jamshidi and Rabiee, 2014). The  $\text{CH}$  and  $\text{CH}_2$  carbons of the main chain are detected around 39 ppm. The two  $\text{CH}_3$  groups of AMPS are detected around 25.92 ppm; the quaternary carbon of the AMPS group was detected at 42.9 ppm, and the  $\text{CH}_2$  of the same AMPS being near the  $\text{SO}_3\text{Na}$  group is detected at 67 ppm. The peak at 128 ppm is assigned to aromatic carbons of the styrene monomer (Baigl et al., 2002; www.unige.ch). The figure is not reproduced here due to the low quality of signal.

In summary, both  $^1\text{H}$  NMR and  $^{13}\text{C}$  NMR confirmed the presence of the three monomers in the polyelectrolyte.

### 2.2.2. Elemental analysis of sulfur, carbon and nitrogen

The tri-copolymer composition was determined by elemental analysis of Carbon, Sulfur and Nitrogen, at the INRAP - Sidi Thabet. The determination of carbon %, sulfur % and nitrogen % was achieved by the apparatus HORIBA JOBINIVON EMIA 220V; Sodium was titrated by atomic emission spectroscopy in aqueous solution at 589 nm by means of Perkin-Elmer AAnalyst 100 device.

The ratios C/S, C/N and C/Na allow us to determine accurately the percentages of acrylamide ( $x\%$ ), styrene ( $y\%$ ) and AMPS ( $z\%$ ). The corresponding elemental analysis of Sulfur,

Carbon Nitrogen and Sodium is listed in Table S.I 1. Moreover, the evaluated relative errors on  $x$ ,  $y$  and  $z$  were respectively 2.5%, 1.3% and 2.8%.

### 2.2.3. Size exclusion chromatography measurements

For the AM54-ST04-AMPS42 tri-copolymer, the molecular weight distributions and average molecular weights were determined by multidetection Size Exclusion Chromatography (SEC) using one SEC line of the Institut Charles Sadron (ICS) - Strasbourg. This line involves a usual HPLC part (Dionex), a refractometer and a multi-angle light scattering apparatus (Wyatt technology) completed by a dynamic light scattering detector. The fractionation was carried out through four Shodex columns based on poly(vinyl alcohol) gel arranged in series. The eluent was a mixture of water and acetonitrile with a volume composition 60–40, respectively, in the presence of 0.1 M  $\text{NaNO}_3$ . Measurements were performed at room temperature using a constant flow rate of  $0.5\text{ ml min}^{-1}$ . Tri-copolymer solution of concentration  $1.2\text{ g L}^{-1}$  was filtered on a  $0.45\text{ }\mu\text{m}$  membrane prior to be injected.

The differential refractometer detector enables determining the concentration of each fraction, while the light scattering detector enables determining the molecular weight of each fraction, the radius of gyration of those associated with large enough molecular weight, as well as the hydrodynamic radius (Fig. 3a).

By considering a refractive index increment value  $dn/dc = 0.134\text{ cm}^3\text{ g}^{-1}$  (Read et al., 2014; <http://www.chemical-book.com>), the analysis of the chromatograms (Fig. 3b) gives the number average molecular weight  $M_N = 347.000\text{ g mol}^{-1}$  and the weight average molecular weight  $M_W = 561.000\text{ g mol}^{-1}$ . The polydispersity index is therefore  $I = M_W/M_N = 1.62$ .

Moreover, it allows determining the various averages of the gyration and hydrodynamic radii  $\langle R_G \rangle$  and  $\langle R_H \rangle$ , respectively. So, for AM54-ST04-AMPS42 they are as follows:

$$\begin{aligned} \langle R_G \rangle_N &= 27.6\text{ nm}; \langle R_G \rangle_W = 38.8\text{ nm}; \langle R_G \rangle_Z = 63.2\text{ nm}, \\ \langle R_H \rangle_N &= 13.6\text{ nm}; \langle R_H \rangle_W = 17.8\text{ nm}; \langle R_H \rangle_Z = 21.8\text{ nm}, \end{aligned}$$

where the indexes  $N$ ,  $W$  and  $Z$  refers to the number, weight and  $z$  averages.

We do not have values for all samples. However measurements for samples such as di-copolymers and homopolymers (not shown here) show that our copolymerization conditions (solvent, catalyst) lead to quite long chains ( $>$  several  $100,000\text{ g mol}^{-1}$ ). We thus expect to be always in semidilute regime  $c > c^*$  ( $\sim 0.00381\text{ g cm}^{-3}$  for AM54-ST04-AMPS42, knowing that  $c^* = \frac{M_w}{\frac{4}{3}\pi N_A \langle R_G \rangle_w^3}$ ), for which chains interpenetrate so that the scattering does not depend on the molecular mass.

## 2.3. Preparation of solutions for scattering measurements

Solutions were prepared by dissolving the dry polyelectrolyte in the solvent. Solvent is  $\text{D}_2\text{O}$  for SANS measurements, in order to get the best contrast, and  $\text{D}_2\text{O}$  as well for SAXS, in order to be exactly in the same solvent. Solutions were let at rest 2 days before scattering measurements. Concentrations  $c_p$  are expressed in moles per liter of the corresponding monomers and range between  $0.04\text{ mol L}^{-1}$  and  $0.68\text{ mol L}^{-1}$ , the most explored being  $0.34\text{ mol L}^{-1}$ .

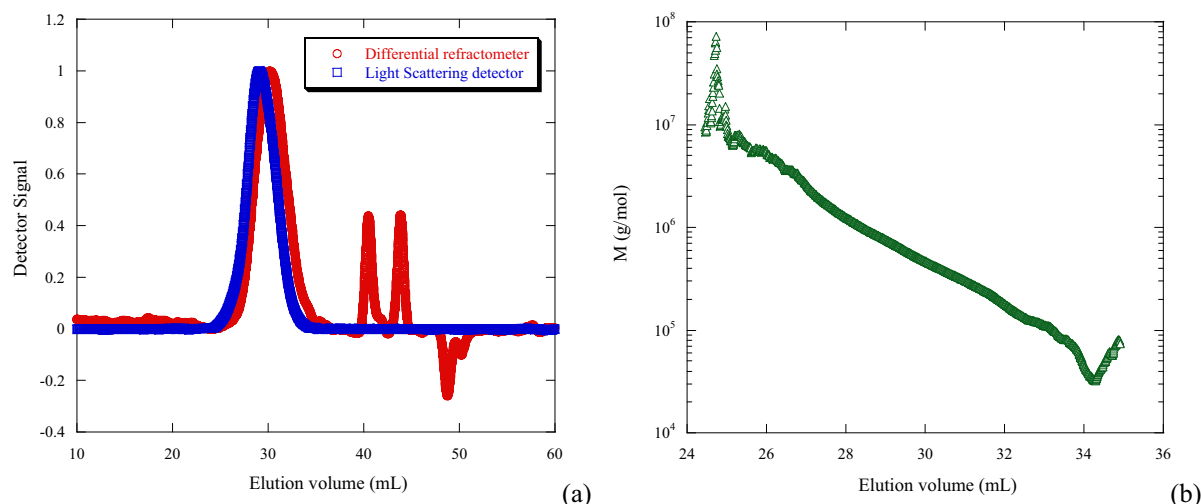


**Figure 3** Chromatograms of AM54-ST04-AMPS42 (a) and the corresponding elution volume dependence of the molecular weight measured from the multi-angle light scattering detector (b).

#### 2.4. Small angle scattering measurements

We use both Small Angle Neutron Scattering and Small Angle X-Ray Scattering to determine the structure of the PE solutions, which will enable useful comparisons.

##### 2.4.1. Small angle neutron scattering (SANS)

SANS measurements were performed on the PACE spectrometer at the Orphée reactor of Laboratoire Léon Brillouin (LLB), CNRS-CEA, Saclay (<http://www-llb.cea.fr>). A range of scattering vector  $q = (4\pi/\lambda) \cdot \sin(\theta/2)$ , where  $\lambda$  is the wavelength of the incident beam and  $\theta$  the scattering angle, between 0.00825 and 0.497  $\text{\AA}^{-1}$  was covered by using the following two settings:  $D = 1 \text{ m} - \lambda = 5 \text{ \AA}$ ,  $D = 5 \text{ m} - \lambda = 6 \text{ \AA}$ . The scattered intensity was recorded by a multidetector with 30 concentric 1 cm wide rings. The response of each ring was normalized to the (flat) incoherent scattering of light water. Samples were contained in 2 mm thick quartz cells. All measurements were done at room temperature.

The recorded intensities were corrected for sample thickness, transmission, and incoherent and background scattering (the solvent contribution). Using direct beam measurements of Cotton method ([Cotton, LLB Web site](#)), the intensities were obtained in absolute units of crosssection per unit volume ( $\text{cm}^{-1}$ ). The general expression of the scattered intensity:

$$I(q) = (\text{cm}^{-1} \text{ or } \text{\AA}^{-1}) = (1/V)d\Sigma/d\omega \\ = 1/V \cdot \left( \sum_{ij} K_i K_j \exp(i\vec{q}(\vec{r}_i - \vec{r}_j)) \right) \quad (1)$$

Here  $V$  is the sample irradiated volume,  $d\Sigma/d\omega$  is the cross section,  $K_i$  ( $\text{cm}$  or  $\text{\AA}$ ) =  $b_i - b_s(V_{\text{mol},i}/V_{\text{mol},s})$ , where,  $b_i$  (resp.  $b_j$ ) is the “scattering length” of a statistical unit  $i$  (resp.  $j$ ) of the polymer, of molar volume  $V_{\text{mol},i}$  (resp.  $V_{\text{mol},j}$ ), and  $b_s$  is the “scattering length” of a solvent molecule of molar volume  $V_{\text{mol},s}$ .  $\vec{r}_i(\vec{r}_j)$  are the spatial positions of two statistical units. One can also define the Scattering Length Density (SLD) difference:

$$K_i/V_{\text{mol},i} = (b_i/V_{\text{mol},i}) - (b_s/V_{\text{mol},s}) \\ = \text{SLD}_i - \text{SLD}_s (\text{cm}^{-2}) \quad (2)$$

In this experiment all chains are labeled with respect to the solvent; here, we dissolve hydrogenated AM<sub>x</sub>-ST<sub>y</sub>-AMPS<sub>z</sub> into D<sub>2</sub>O. We define the scattering lengths for each type of statistical unit,  $b_{\text{AM}}$ ,  $b_{\text{ST}}$  and  $b_{\text{AMPS}}$ .

The average squared root of the contrast,  $\langle K_{\text{PEL}} \rangle$ , (sometimes called “contrast length”) has been calculated for the different copolymers using the formula:

**Table 2** Values of the molar volumes and contrasts of some of the samples.

AM (x)	ST (y)	AMPS (z)	$V_{\text{mol}}$ ( $\text{cm}^3$ )	$b_{\text{neutronsTri-copolymer}}$ (cm)	$K_{\text{neutrons}}^2$ ( $\text{cm}^2$ )	$b_{\text{X-ray without Na condensation}}$ (cm)	$K_{\text{X-ray without Na condensation}}^2$ ( $\text{cm}^2$ )
17	44	39	104.74	$2.75 \cdot 10^{-12}$	$6.83 \cdot 10^{-23}$	$2.08 \cdot 10^{-11}$	$1.99 \cdot 10^{-23}$
40	04	56	100.28	$2.84 \cdot 10^{-12}$	$5.94 \cdot 10^{-23}$	$2.20 \cdot 10^{-11}$	$4.15 \cdot 10^{-23}$
23	06	71	114.05	$3.16 \cdot 10^{-12}$	$7.81 \cdot 10^{-23}$	$2.53 \cdot 10^{-11}$	$5.64 \cdot 10^{-23}$
54	04	42	88.31	$2.56 \cdot 10^{-12}$	$4.53 \cdot 10^{-23}$	$1.91 \cdot 10^{-11}$	$2.92 \cdot 10^{-23}$
10	50	40	108.45	$2.81 \cdot 10^{-12}$	$7.39 \cdot 10^{-23}$	$2.13 \cdot 10^{-11}$	$1.96 \cdot 10^{-23}$
45	06	49	95.24	$2.71 \cdot 10^{-12}$	$5.33 \cdot 10^{-23}$	$2.07 \cdot 10^{-11}$	$3.46 \cdot 10^{-23}$
17	17	66	115.00	$3.13 \cdot 10^{-12}$	$8.05 \cdot 10^{-23}$	$2.48 \cdot 10^{-11}$	$4.82 \cdot 10^{-23}$
26	23	51	105.03	$2.86 \cdot 10^{-12}$	$6.70 \cdot 10^{-23}$	$2.21 \cdot 10^{-11}$	$3.28 \cdot 10^{-23}$

$$\begin{aligned} \langle K_{\text{PEL}} \rangle (\text{cm or } \text{\AA}) &= x \cdot b_{\text{AM}} + y \cdot b_{\text{ST}} + z \cdot b_{\text{AMPS}} \\ &\quad - b_s((x \cdot V_{\text{mol,AM}} + y \cdot V_{\text{mol,ST}} \\ &\quad + z \cdot V_{\text{mol,AMPS}}) / V_{\text{mol,s}}) \end{aligned} \quad (3)$$

The molar volumes of the three repeat units were taken from experimental data. Table 2 shows the different values of contrasts obtained for the different triplets ( $x, y, z$ ) and different molar volumes. The choice we made for neutrons, should in principle be kept for X-rays. One open problem is the role of the counterions, (i) in their actual contribution to the volume, as well as (ii) in the extent of their condensation. This will be discussed below. Finally we define the quantity  $S_T(q)$  as the total scattering function, by dividing the intensity  $I$  by the average contrast  $\langle K_{\text{PEL}}^2 \rangle$ :

$$S_T(q) = I(\text{cm}^{-1}) / \langle K_{\text{PEL}}^2 \rangle (\text{cm}^2) \quad (4)$$

where  $S_T(q)$  is in  $\text{cm}^{-3}$  or  $\text{\AA}^{-3}$  as given in this paper.

#### 2.4.2. Small angle X-ray scattering (SAXS)

The structure of our polyelectrolyte has been also measured by Small Angle X-ray Scattering (SAXS) at ICS, Strasbourg, with a diffractometer developed by Molecular Metrology (Elexience in France) that uses a Rigaku Micromax 007HF generator with a copper-rotating anode. The wavelength of the incident X-ray beam is  $\lambda = 1.54 \text{ \AA}$ . This diffractometer operates with a pinhole collimation of the X-ray beam focused by a multi-layer optic designed by Osmic and a two-dimensional gas-filled multiwire detector. The sample-detector distance was set at  $D = 0.7 \text{ m}$ , leading to a range of scattering vectors  $q$  ( $q = (4\pi/\lambda) \sin(\theta/2)$ ) covered by the experiment  $0.01 \text{ \AA}^{-1} < q < 0.32 \text{ \AA}^{-1}$ . Cells of 1 mm thickness and calibrated Mica windows were used as sample holders. Measurements were performed at room temperature.

Data were treated according to a standard procedure for isotropic SAXS. After radial averaging, curves were corrected from electronic noise of the detector, empty cell, absorption and sample thickness. A  $^{55}\text{Fe}$  source was used for the

corrections of geometrical factors and detector cell efficiency. A Silver behenate sample allowed the  $q$ -calibration and the normalization to the unit incident flux was obtained using Lupolen, or water, as standard sample, giving then measurements in absolute scale ( $\text{cm}^{-1}$  as well as for SANS) and this will be used below. Finally, the scattered intensities were corrected from the scattering of the solvent. This last subtraction accounted for the presence of free counterions in the solvent.

The scattering profiles are plotted as intensity  $I(q)$  ( $\text{cm}^{-1}$ ) versus  $q$ , or  $S_T(q)$  ( $\text{cm}^{-3}$  or  $\text{\AA}^{-3}$  after division of  $I(q)$  by  $K_N^2$  or  $K_X^2$ , in  $\text{cm}^2$ ) versus  $q$ .

### 3. Results

Let us first describe rapidly the set of the  $S_T(q)$  scattering profiles of the tri-co-polyelectrolyte semidilute aqueous solutions, summarized in Table 3: they all show the presence of a polyelectrolyte peak in the structure function, attributed to a correlation hole according to the theoretical models (de Gennes et al., 1976; Dobrynin and Rubinstein, 1999) and observed experimentally by Neutron scattering (Nierlich et al., 1979) and by X-ray scattering (Essafi et al., 1994) on classical polyelectrolytes such as the fully charged polystyrene sulfonate. Note also that they display an upturn at very low  $q$ . This upturn has been remarked many times since long ago (Nierlich et al., 1979). It is not fully explained, but not related to hydrophobicity only. Several papers have considered this problem in more detail, including the case of polystyrene-co-styrene sulfonate (Essafi et al., 2014). We will not comment it further here since it will not show important variations.

#### 3.1. A methodology point: comparison of SAXS/SANS

Let us now compare the SANS and SAXS profiles of the same tri-co-polyelectrolyte. Fig. 4 shows the comparison for AM17-ST44-AMPS39. For that we divide SANS as well as SAXS intensities by the square contrast values, here  $K_N^2 = 6.83$

**Table 3** Copolymers, concentrations and scattering methods used.

AM (x)	ST (y)	AMPS (z)	Polyelectrolyte concentration (mol L <sup>-1</sup> )	Polyelectrolyte mass fraction %	Salt concentration (mol L <sup>-1</sup> )	Radiation used	Transmission
17	44	39	0.34	4.31	10 <sup>-5</sup>	X-ray and neutron	0.79
			0.34	4.28	0.1	Neutron	0.82
				4.23	0.34		0.80
			0.04, 0.08, 0.17, 0.45, 0.68	0.53, 1.03, 2.20, 5.62, 8.26	10 <sup>-5</sup>	X-ray and neutron	0.78, 0.81, 0.78, 0.80, 0.78
54	04	42	0.34	4.06	10 <sup>-5</sup>	X-ray and neutron	0.83
			0.04, 0.08, 0.17, 0.68	0.49, 0.98, 2.06, 7.83	10 <sup>-5</sup>	X-ray	–
45	06	49	0.34	4.4	10 <sup>-5</sup>	X-ray	–
10	50	40	0.34	4.41	10 <sup>-5</sup>	X-ray and neutron	0.74
26	23	51	0.34	4.64	10 <sup>-5</sup>	X-ray and neutron	0.78
40	04	56	0.34	4.69	10 <sup>-5</sup>	Neutron	0.78
17	17	66	0.34	5.30	10 <sup>-5</sup>	X-ray	–
23	06	71	0.34	5.36	10 <sup>-5</sup>	X-ray	–
23	04	73	0.34	4.87	10 <sup>-5</sup>	Neutron	0.76
20	55	25	0.34	3.79	10 <sup>-5</sup>	X-ray	–
05	67	28	0.34	4.01	10 <sup>-5</sup>	X-ray (Demixed solution)	–

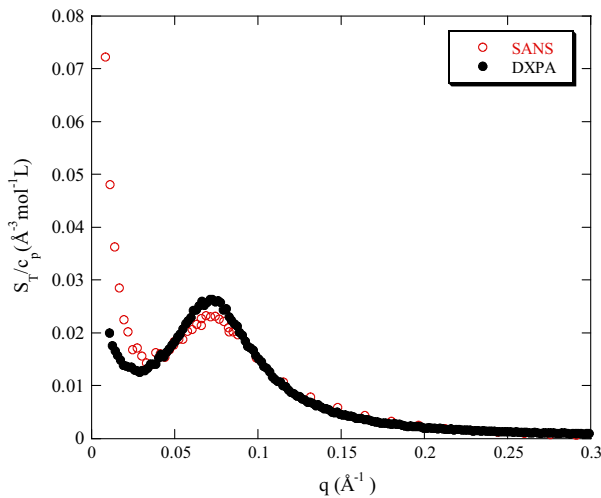


**Figure 4** Comparison of the SANS and SAXS profiles for a tri-co-polyelectrolyte AM17-ST44-AMPS39,  $c_p = 0.34 \text{ mol L}^{-1}$ . Both scattered intensities are divided by the contrasts, equal to  $6.83 \cdot 10^{-23} \text{ cm}^2$  for SANS and chosen equal to  $1.99 \cdot 10^{-23} \text{ cm}^2$  for X-rays, in the absence of condensation. The units of  $S_T(q)/c_p$  are in  $\text{\AA}^{-3} \text{ mol}^{-1} \text{ L}$ .

$10^{-23} \text{ cm}^2$  for SANS and  $K_X^2 = 1.99 \cdot 10^{-23} \text{ cm}^2$  for X-rays. The first is the value chosen in Table 2 for SANS for this tricopolymer composition ignoring the neutron scattering from sodium counterions (Dubois and Boué, 2001). The second is also the contrast value with a condensed counterions fraction equal to zero. This is not far from the fraction of condensed Na ions ( $f_{chim} - f_{eff}$ ) = 39–36% = 3%, calculated assuming Manning condensation, for which  $f_{eff} = a/l_B = 36\%$  ( $a$  is the length of AMPS repeat unit).

The difference found above between SAXS and SANS profiles is within the error limits due to normalization, evaluation of the scattering volumes and partial molar volume. Superposing the maxima for neutron and X-rays is possible for  $K_X^2 = 2.3 \cdot 10^{-23} \text{ cm}^2$ . It corresponds to a quite different value of  $f_{eff} = 36\%$ , whereas we remain within the error limits. In summary, it is not possible to evaluate further the counterion binding from a SANS/SAXS comparison. For the sake of simplicity, we will use in the following the values of  $K_X^2$  without condensed counterions.

Another interesting point is that the heterogeneity of the chemical composition along the chain, has no influence. Indeed the 3 different types of statistical units, AM, ST, and AMPS have different scattering length, and hence different individual contrast but if their distribution among all different chains is random, the system is equivalent to all chains with all monomers having the same average contrast. This is consistent with the shape of all curves and with the fact that the scattering of neutrons and that of X-rays are quite close when both have been measured. Moreover, this supports the assumption of really random statistical copolymerization.

Lastly, the low  $q$  upturn is more pronounced for SANS. This can be due to the angular width of the neutron incoming beam, which in this setting is larger than for X-rays. This produces the enlargement of the upturn commonly observed for most of the polyelectrolyte solutions which is still an open question in the field.

### 3.2. Effect of the hydrophobic styrene content at constant chemical charge fraction

Let us first follow the effect of the hydrophobicity, controlled by the amount of polystyrene repeat unit, ST, hydrophobic, in the backbone of the polyelectrolyte and of AM (hydrophilic), at a constant chemical charge fraction (AMPS content) on the polyelectrolyte structure properties. That can be monitored by both SANS and SAXS. We use the values of  $K_X^2$  ( $K_N^2$ ) calculated by neglecting the condensed counterions.

#### 3.2.1. For a constant chemical charge fraction $f_{chem} \approx 40\%$

Fig. 5a shows  $S_T(q)$  obtained from SAXS at a polymer concentration  $c_p = 0.34 \text{ mol L}^{-1}$ , for three tri-co-polyelectrolytes of chemical charge fractions (AMPS content  $f_{chem} = z$  close to 40%) and of two quite distinct hydrophobic contents. Compared to AM17-ST44-AMPS39 (already shown in Fig. 4), the most hydrophilic AM54-ST04-AMPS42 copolymer shows an increase in the peak position  $q^*$ , with a broader peak and a very strong decrease in the peak intensity at  $q^*$ ,  $I(q^*)$ . On the reverse the most hydrophobic polymer (where  $y$  is 50% and  $x$  only 10%) shows an even smaller  $q^*$  value and a much stronger peak intensity  $I(q^*)$ . The same trend is observed with SANS (Fig. SI.1).

These results simply show that the solvent quality has a great influence on the solution properties. Depending on the proportion of the three monomers, the chain follows a continuous transition, from a partly pearl necklace collapsed conformation (Dobrynin and Rubinstein, 1999), to a stretched one described within the isotropic model through the scaling approach (de Gennes et al., 1976; Dobrynin et al., 1995). This is in agreement with the previous result (Essafi et al., 1995) found on three different di-copolymers, with the same  $f_{chem} = 55\%$ : poly(ST-co-SNa), poly(ST-co-AMPS) and poly(AM-co-AMPS). But here with tri-copolymers, we observe a combined contribution to hydrophobicity of both ST (undoubtedly positive) and AM (null or negative, see in the Discussion a comparison between tri-copolymer and some di-copolymers).

#### 3.2.2. For larger charge fractions $f_{chem}$

Note first that larger charge fraction means necessarily smaller styrene fraction  $y$ , since the sum of the neutral monomers decreases as  $f_{chem}$  increases:  $y = 1 - f_{chem} - x < 1 - f_{chem}$ .

For a constant charge fraction  $f_{chem} \approx 50\%$ , insert of (Fig. 5a) for SANS shows that the peak position does not vary strongly as the styrene content decreases from 23% to 04% (there is however unexplained decrease of 30% of the intensity).

For a constant charge fraction  $f_{chem} \approx 70\%$  (see SI.2), the available styrene fractions are bound to be even lower:  $y$  is equal to 17 and 6. The effect is even less pronounced, as seen by SAXS on  $S_T(q)/c_p$ .

In summary of this sub-section, when the styrene fraction is below 20%, we reach a plateau regime where the chain behaves as hydrophilic. Note that the hydrophobicity can also be balanced either by the increase in charge fraction, or by the presence of non-negligible amount of AM.

In summary of Section 3.2, the effect of the hydrophobicity is moderate for styrene contents until 25%, while for styrene contents approaching 50% or larger, it is very significant.

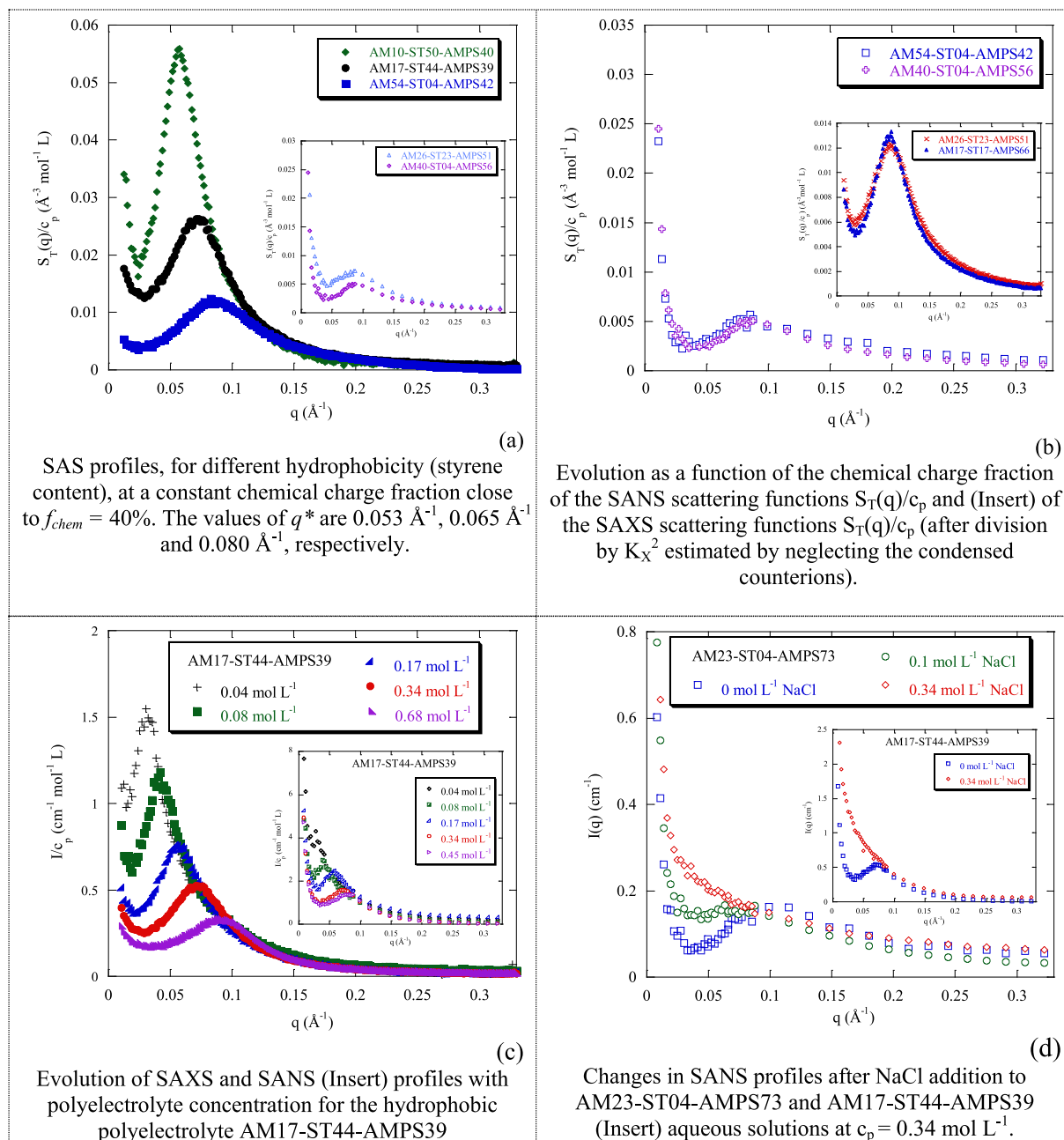


**Figure 5** Evolution of the scattering of tri-co-polyelectrolytes as a function of hydrophobicity (a), chemical charge fraction (b), polyelectrolyte concentration (c) and added salt (d).

The maximum styrene content reached for a soluble copolymer was for AM20-ST55-AMPS25, for which  $q^*$  went as low as  $0.055 \text{ \AA}^{-1}$  (see Fig. S.I.3). For even larger content, e.g. for AM05-ST67-AMPS28, the copolymer was not soluble any more: the aqueous solution was demixed, as indicated by a strong upturn in the scattering, and the vanishing of the peak (see Fig. S.I.3).

In the Discussion, we will focus on a more detailed comparison with other systems formerly reported in the literature (Fig. 7), using the  $q^*$  values, which sheds light on finer differences.

### 3.3. Effect of the chemical charge fraction and acrylamide content at constant hydrophobic styrene content

Using the same set of data, we can also analyze the effect of the chemical charge fraction at constant hydrophobic content.

#### 3.3.1. Low styrene content ( $y$ close to 4%): the hydrophilic case

Here we deal with close-to-hydrophilic polyelectrolytes. SANS in (Fig. 5b) shows that  $q^*$  increases only very slightly when increasing  $f_{chem}$  from 42% to 56% (correlatively,  $S_T(q^*)$  varies

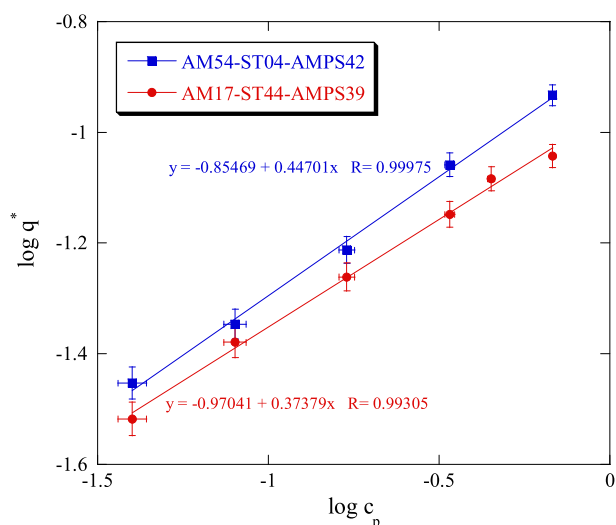


**Figure 6** Log-log plot of  $q^*$  as a function of  $c_p$ , for a strongly hydrophobic and a quasi-hydrophilic polyelectrolyte.

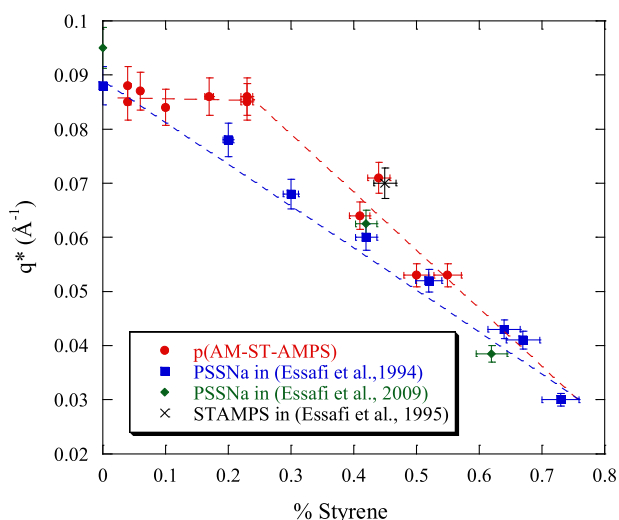


**Figure 7** Variation of  $q^*$  with styrene content  $y$  in different copolymers at  $c_p = 0.34 \text{ mol L}^{-1}$ , compared with data PSSNa (Essafi et al., 1994), PSSNa (Essafi et al., 2009) and STAMPS (Essafi et al., 1995).

weakly). There is only a small further expansion of the chain; SAXS (before correction by the contrast Fig. S.I.4 and after correction by the contrast, Fig. S.I.5) is quite close to SANS evolution for three copolymers: for a charge fraction  $f_{chem}$  change from 42% to 49%, here also  $S_T(q^*)$  varies very slightly (the X-ray accuracy enables also to see that the relative peak width at half maximum  $\Delta q/q^*$  stays constant around 0.95).

On the same figure (Fig. S.I.5), we see that passing to larger AMPS content, 71%,  $q^*$  increases a little (and  $S_T(q^*)$  decreases correlatively). The chain is slightly stretched. This is opposite to two usual expectations:

- c.i. condensation, which should balance the increase by bringing  $f_{eff}$  back from 70% to 36% (as for partially charged hydrophilic poly(AM)<sub>(1- $f_{chem}$ )</sub>-co-(AMPS) <sub>$f_{chem}$</sub>  (Essafi et al., 1999)),

- a  $z$  increase induces a decrease of AM content, which should increase the chain hydrophobicity.

However, it is a small variation. We can also find another explanation, if we note that AMPS sequences with condensed counterions are themselves hydrophilic.

*Scattered intensity at zero angle*  $S_T(q \rightarrow 0)$ . This quantity is also linked to electrostatic charge effects. Minute variations can be detected using the “plateau value” just before the upturn when  $q$  tends to zero, id est in practice the minimum of the curve. This is possible for the curve of Fig. 5b in particular. This enables a direct measurement of the amount of free counterions which is related to the osmotic compressibility  $\partial c_p / \partial \pi_{osm}$  by the equation (Essafi et al., 2005):

$$S_T(q \rightarrow 0) = kTc_p \frac{\partial c_p}{\partial \pi_{osm}} = \frac{c_p}{\frac{f_{eff}}{2}} \quad (5)$$

$\pi_{osm}$  is the osmotic pressure. The plateau height ( $0.000255 \text{ \AA}^{-3} \text{ mol}^{-1} \text{ L}$ ) is kept unchanged (Fig. 5b) whatever the electric charge rate, which means that the osmotic compressibility is constant with  $f_{chem}$  indicating a constant number of free counterions, giving  $f_{eff}$  of 0.47, regardless of  $f_{chem}$ . This value is slightly overestimated than that measured by osmotic pressure measurements for hydrophilic polyelectrolytes in aqueous solution (Essafi et al., 2005) where  $f_{eff}$  was found to be 0.36. This difference should be corrected from the uncertainty of  $S_T(q \rightarrow 0)$  measurement in those experimental conditions. This behavior ( $S_T(q \rightarrow 0)$  is constant) is consistent with the quasi-constant peak position  $q^*$ , and was formerly reported for poly(AM)<sub>(1- $f_{chem}$ )</sub>-co-(AMPS) <sub>$f_{chem}$</sub>  (Essafi et al., 1999).

With our correction for contrast, which does not account for condensed counterions ( $\text{Na}^+$ ) (Table 2), variation of the maximum is consistent with the one of  $q^*$ . This is satisfactory. However we just want to point that accounting for all condensed counterions would not modify the ranking of the peak intensities: it is therefore not possible to decide about condensation on these premises.

### 3.3.2. Larger amount of styrene $y = 17\%$ and $23\%$ : the quasi-hydrophilic case

Insert of Fig. 5b shows that in such cases the position of the characteristic polyelectrolyte peak  $q^*$  (for SAXS) does not yet vary, and still amounts to the largest values found for the most hydrophilic case ( $y = 4\text{--}6\%$ ). The two curves  $S_T(q)/c_p$  nicely overlap.

In summary, the tri-co-polyelectrolytes behave as hydrophilic ones for a negligible amount styrene content  $y \approx 4\text{--}6\%$ , but also for non-negligible styrene content  $y$  of about 20%. In this case, even the change of charge fraction from 51 to 66% has no effect. All this will be commented in the Discussion section.

### 3.3.3. Hydrophilic polymer fraction versus chemical charge fraction

Finally, we can go deeper into the question: for a given styrene content, and a different rate of AMPS, which of the AMPS (electrostatic interaction) or AM (hydrophobicity reduction) determines the solution structure? On top of results listed just above, another way to answer this question is given by comparisons at a larger ST content: AM17-ST44-AMPS39 with AM02-ST41-AMPS57 (very low AM content). For the latter

(see Fig. SI.6),  $q^*$  is clearly smaller ( $0.063 \text{ \AA}^{-1}$ , instead of  $0.073 \text{ \AA}^{-1}$ ). Hence, AM brings more hydrophilicity than charged AMPS units when the global hydrophobicity is large. At low hydrophobicity, the “hydrophilizing” effect of AM will be made clear when looking more closely at the variation of  $q^*$  in (Fig. 7), see below.

### 3.4. Effect of polyelectrolyte concentration

Another marker of hydrophobicity is the variation of  $q^*$  with polymer concentration  $c_p$ . It was studied by SANS and SAXS in a range between  $c_p = 0.04$  and  $c_p = 0.68 \text{ mol L}^{-1}$ . Fig. 5c shows the evolution of SAXS and SANS (Insert) profiles with polyelectrolyte concentration for the hydrophobic polyelectrolyte AM17-ST44-AMPS39. The same effect of  $c_p$  is observed as  $c_p$  increases: the peak position  $q^*$  shifts to higher  $q$  values and the normalized scattered intensity per monomer decreases. For the hydrophilic polyelectrolyte AM54-ST04-AMPS42, the evolution with  $c_p$  of SAXS profiles (Fig. SI.7) looks similar at first sight.

However, differences linked with hydrophobicity arise from a more quantitative analysis, namely the variation of  $q^*$  as a function of  $c_p$ : Fig. 6 shows that  $q^*$  scales as  $c_p^{-\alpha}$  for both polyelectrolytes, but with distinct exponents  $\alpha$ :  $0.37 \pm 0.02$ , for the hydrophobic polyelectrolyte, and  $0.44 \pm 0.03$ , for the hydrophilic one. This evolution indicates that the structures of both polyelectrolytes are different; the system is likely to behave as a solution of elongated chains in the case of hydrophilic polyelectrolyte (as in the string controlled limit), as well known, and as a solution of charged beads in the case of hydrophobic polyelectrolyte (collapsed spheres or bead controlled limit).

Our findings here are very similar to the ones for the model partially sulfonated PSS in water: the total structure function was measured by SAXS and SANS and it was found that  $q^*$  was scaling as  $c_p^{-\alpha}$ , with  $\alpha$  decreasing from 0.5 to less than 0.4 when reducing the chemical charge fraction of the chain  $f_{chem}$  (Essafi et al., 1994; Spiteri, 1997). Later, this was also observed by Baigl et al., through both SAXS and atomic force microscopy studies (Baigl et al., 2003a,b; Dan Qu et al., 2003).

### 3.5. Effect of ionic strength

Monovalent salt addition is expected to screen the repulsive Coulombic interactions, which makes the polyelectrolyte “peak” vanish. The scattered intensity at very low  $q$  (up to the position of peak) increases with salt concentration  $c_s$ , reflecting larger long-range concentration fluctuations and thus an increase in the compressibility of the system.

This is seen in Fig. 5d enabling to observe the effect of the hydrophobicity. For the more hydrophilic polyelectrolyte, with a smaller added salt concentration of  $0.1 \text{ mol L}^{-1}$ , the peak remains present at the foot of the low  $q$  upturn, but even for  $c_p = 0.34 \text{ mol L}^{-1}$  and  $c_s = 0.34 \text{ mol L}^{-1}$  NaCl ( $c_s/c_p = 1$ ), the polyelectrolyte peak is slightly visible. For the hydrophobic case, Insert of Fig. 5d shows that a ghost of a peak is hardly visible; the sensitivity to salt is higher, inducing stronger concentration fluctuations (however there is no demixing). This reactivity is even more visible with yet no phase separation for the most hydrophobic polyelectrolyte, and  $1 \text{ mol L}^{-1}$  NaCl ( $c_s/c_p \sim 3$ ), in Fig. SI.8.

Very similar observations have been made by Essafi et al. (1999) on AM-AMPS, and by Essafi et al. (1994) and Spiteri et al. (2007) on partially sulfonated PSSNa. Indeed the scattering behavior of tri-copolymers is akin to the one of partially sulfonated polystyrene for polyelectrolyte concentration variation as well as salt addition. Let us now make more precise comparisons.

## 4. Discussion. Comparison with P-S-co-SSNa

This discussion is mainly devoted to the use of scattering results to answer two questions:

- Is radical copolymerization a good way of getting polyelectrolytes with the same behavior than partially sulfonated polystyrene, i.e. the pearl necklace conformation ?
- Does the ability to have hydrophobic content partly independent from the chemical charge content give more information on the hydrophobicity/hydrophilicity balance ? more precisely: how does tuning chemical charge balance compact conformation, knowing that the latter controls in fine the effective electric charge, through counterions condensation phenomena ?

But before to physical discussion, let us briefly conclude the combined use of SANS and SAXS on these systems.

### 4.1. Methodology: from SANS to SAXS

The scattering functions  $S_T(q)$  from SANS obtained after normalization to the contrast  $K_N^2$  can be made superposed on those from SAXS after normalization to a contrast  $K_X^2$ . Calculating  $K_X^2$  without accounting for the  $\text{Na}^+$  counterions, the result is satisfying. Including the counterions in the calculation does not change the ranking of the contrast values for the different copolymers neither makes strong changes of  $S_T(q)$ . Hence, estimating condensation by comparisons between Neutron and X-rays measurements is delicate here and requires a larger and dedicated set of data to conclude. Anyhow, sodium counterions ( $\text{Na}^+$ ) are not the main origin of the SAXS contrast for extended or partly contracted linear chains.

### 4.2. Global comparison with former scattering from pearl-necklace-like systems

The literature mostly concerns partially sulfonated polystyrene (Essafi et al., 1999, 1994, 1995, 2009) which indeed exhibited such pearls (see Introduction). Except for the unique case of ZAC measurement of  $S_1(q)$ , we can assume that most of the accessible information can be summarized by the values of  $q^*$ .

The variation of  $q^*$  values with styrene content, is shown in Fig. 7 for both di-copolymers and tri-copolymers. Variation with other parameters (AM or AMPS content) more scattered, can be seen in Supporting Information (see Figs. SI.9 and SI.10). The  $q^*$  of tri-copolymers show, in gross approximation, a variation with styrene content rather close to the one for “bi-copolymers” case, namely poly(styrene-co-sodium styrene sulfonate), and for poly(styrene-co-sodium-2-acrylamido-2-methylpropane sulfonate) for one point. However:

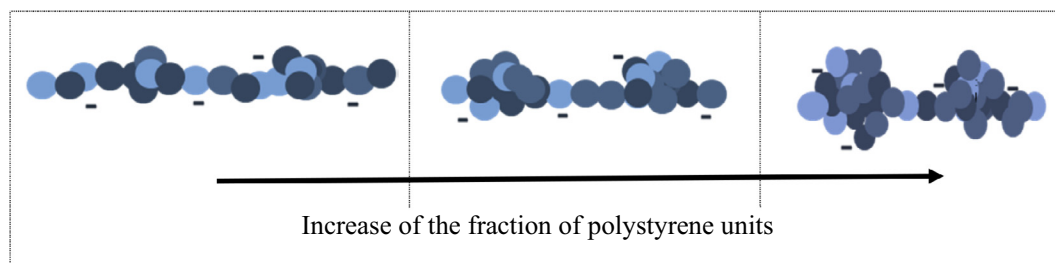


**Figure 8** Proposed evolution of the tri-co-polyelectrolytes conformation in aqueous solution as the hydrophobicity increases (% styrene increase).

- a clear difference appears below 20% ST content, where  $q^*$  stays quasi-constant to the value at zero ST content. For these points, the AM content (see Table 3) is large, while the AMPS is always larger than the Manning threshold. This evidences an hydrophilic effect of AM, while AMPS content effect does not vary. Reciprocally, in the same interval we also notice a lower point in Fig. 7: it indeed corresponds to a much smaller AM content.
- when ST approaches 40% ST content, for all samples where AMPS remains larger than 36%, AM is bound to be reduced: however its effect is still observed since  $q^*$  remains only slightly higher than for the di-copolymers, for two other pairs of points.
- finally, above 55% ST content, AM content is even more decreased and there is no more hydrophilic effect: the  $q^*$  values overlap those of the di-copolymers. We note that for the largest styrene content, 67%, precipitation is observed.

A proposed evolution of the conformation of the tri-co-polyelectrolytes in aqueous solution as the hydrophobicity increases (% styrene increases) is given in Fig. 8 below.

Let us now attempt to more quantitative considerations using a theoretical model.

#### 4.3. Detailed comparison with the Dobrynin - Rubinstein (DR) model

As briefly recalled in Introduction, the different models for strongly charged hydrophobic polyelectrolytes result in a different variation of  $q^*$  as a balance of a bad solvent effect and electrostatic repulsion. We will use specifically for our discussion the DR model, which we believe is the most relevant. The chain is a random walk of correlation blobs of size  $\xi$ , each of which is an extended configuration of electrostatic blobs of  $g_e$  monomers inside the blob diameter  $D$ . Therefore  $\xi$  is close to a geometrical distance between rod-like strands of chains and depends on their effective linear density of segments ( $g_e/D$ ), which we will define as equal to  $B/a$ , defining  $B$  as in (Dobrynin et al., 1995) and  $a$  is the monomer size:

$$\xi \propto \left( \frac{B}{c_p a} \right)^{1/2} \quad (6)$$

In the case of poor solvent, if we stay in the string-controlled regime,  $q^*$  will still be related to the inverse blob size, and one can introduce the corresponding expression of  $B$  which depends on the normalized distance  $\tau$  ( $\tau = \frac{\Theta - T}{\Theta}$ ) to the theta temperature  $\Theta$  (Dobrynin and Rubinstein, 1999):

$$q^* \propto \left( \frac{2\pi}{\xi} \right) \propto \left( \frac{(\Theta - T)}{\frac{l_B}{a} f_{eff}^2} \right)^{-1/4} c_p^{1/2} \propto \left( \frac{\tau}{\frac{l_B}{a} f_{eff}^2} \right)^{-1/4} c_p^{1/2} \text{ for } T < \Theta \quad (7)$$

The DR model has four main characteristics at the light of which we can discuss our results.

#### – 1/A specific class of hydrophobic polyelectrolytes

The DR model describes a class of non-associative hydrophobic polyelectrolyte. The chains repel each other in solution. This is what observed in our study (for which hydrophobic content (styrene) is never larger than 50%): the solutions stayed clear and did not show any increase of viscosity. The scattering shows a clear repulsion, via the existence of a peak, which can be characterized via the variation of  $q^*$ .

#### – 2/A specific behavior with polyelectrolyte and salt concentration

The salt effect on scattering, which is similar to the one for hydrophilic polyelectrolyte, is also in favor of independent chains with well-defined charge, as discussed just above.

The variation of  $q^*$  with  $c_p$  predicted by DR model is a power  $c_p^\theta$  in Eq. (6). However, there can be crossover between the semidilute ( $c_p^{1/2}$ ) and the dilute regime ( $c_p^{1/3}$ ). Moreover, after the formation of pearls, a crossover is predicted between a string controlled and bead controlled regime. We observed a power law  $q^* \sim c_p^{0.37 \pm 0.02 - 0.45 \pm 0.03}$ , close to what was also found for PS-co-SSNa solutions, which showed pearl necklace behavior conformation (SANS-ZAC measurements).

#### – 3/A balance between hydrophobicity and hydrophilicity

The expression of  $q^*$  (Eq. (7)) rules a balance between electrostatic energy ( $l_B/a$ ),  $f_{eff}^2$  and solvent quality  $\tau = \frac{(\Theta - T)}{\Theta}$ . The first term is linked to the effective charge along the backbone. In the context of Manning-Oosawa theory, the effective charge is expressed as follows:

$$f_{eff} = \frac{a}{|Z|l_B} \quad (8)$$

where  $a$  is the monomer size as already defined,  $Z$  the charge of the ion before condensation ( $Z = 1$  in our case), and  $l_B$  the Bjerrum length:

$$l_B = \frac{e^2}{4\pi\epsilon\epsilon_0 k_B T} \quad (9)$$

with  $T$ : the temperature in Kelvin;  $k_B$ : Boltzmann constant =  $1.38 \cdot 10^{-23} \text{ J K}^{-1}$ ;  $\epsilon$ : the relative dielectric constant

of the medium (solvent).  $\epsilon_0$ : is the vacuum permittivity,  $e$ : elementary electrostatic charge =  $1.6 \cdot 10^{-19}$  C. In water at 25 °C,  $\epsilon = 78$  and so  $l_b = 7 \text{ \AA}$ .

**Let us evaluate  $f_{eff}$  in our system.** This is equivalent to consider Manning condensation:

- if we consider separately each of the AMPS sequences, with  $a \sim 2.5 \text{ \AA}$ , Manning condensation will reduce each of their charge by a factor  $2.5/7 \approx 36\%$ , so the global effective charge rate will be  $f_{eff} \approx 0.36 z/(x + y + z)$ .
- if on the contrary we consider the whole sequence, since the segment length  $a$  is very close for the three polymers PAM, PAMPS and PS, the Manning threshold reduces the charge rate to 36% over the full copolymer length (as long as the AMPS monomers fraction is larger than 36%, which is the case here). The total effective charge is 36%, independent of the AMPS fraction  $z$  ( $z/(x + y + z) > 0.36$ ).

Note that here we consider the charge fraction before the chain contraction (additional condensation may occur later due to the compacity of the chain, or around the pearls, and reduce the final value of  $f_{eff}$ , as observed).

**Let us now evaluate the solvent quality  $\tau$ :** Since Styrene is strongly hydrophobic, the slight difference in hydrophilicity brought by AM and hydrophilicity brought by AMPS could be neglected in first approximation and the simplest is to assume that  $\tau = \frac{(\theta-T)}{\theta}$  is driven by the Styrene content. Thus from Eqs. (7) and (8) we can check whether  $q^*$  is simply driven by a ratio  $R$  of Styrene content ( $\tau^{-1/4}$ ) over the AMPS content (electrostatics,  $f_{eff}^{-1/4}$ ).

However, while Fig. 7 shows a strong effect of Styrene (ST) content as pointed above, it also displays a specificity of the tri-copolymers values of  $q^*$  with high AM content on (Fig. 7), as described above. The possible loss of hydrophilicity brought by the decrease in AMPS is masked by the increase in AM. The solubility is more improved by the mixing of PS units with hydrophilic AM units than with AMPS units:  $\tau$  is driven by the Styrene content but also by the AM content. This agrees with the fact that polyacrylamide is quite hydrophilic ( $\chi \sim 0.5$  (Li et al., 2012; Sen et al., 1999)). AMPS does not seem dominant on  $\tau$ . Its role is mostly to bring electric charges but because of condensation, the charge rate brought remains 36% for all our samples.

#### – 4/A pearl necklace conformation

Such conformation is the main originality of DR model. Unfortunately, conformation can only be evidenced using Zero Average Contrast, which requires deuteration of some of the tri-copolymers. However, we can propose, inferring from the strong similarities with the PS-co-SSNa that such conformation is present for these tri-co-polyelectrolytes.

## 5. Summary and conclusion

Small Angle Scattering study on poly(acrylamide-co-styrene-co-sodium-2-acrylamido-2-methylpropane sulfonate), AMx-STy-AMPSz, semidilute aqueous solutions, with the particularity that the electric/chemical charge fraction and the hydrophobicity are not directly correlated, has been achieved using SANS and-or SAXS. Normalization of the related

scattered intensities to either the neutron or the X-ray contrast leads to scattering functions  $S_T(q)$  that superpose. This occurs within experimental uncertainty, which does not enable to discriminate between the existence and absence of counterions condensation via its consequence on the contrast.

The interpretation of the scattering is that the structure evolves continuously from a collapsed conformation to an elongated one (the latter is usually observed for null content of hydrophobic units), as the styrene content is decreased. Indeed, the polyelectrolyte peak is displaced to higher  $q$  values, the scattered intensity at zero angle and the height of the peak decrease, and the peak widens, until to reach the behavior of a classical hydrophilic polyelectrolyte.

It is particularly interesting to make comparisons with di-copolymers studied formerly, associating Styrene to Styrene sulfonate, or AMPS, through  $q^*$ . For the tri-copolymers:

- There is no dominant chemical charge effect through AMPS content, except at very low chain hydrophobicity. This is probably because  $f_{chem}$  is always above the threshold for Manning condensation, which levels the actual charge rate at a constant value (moreover, after contraction, additional condensation should occur). It would be interesting to check further how much more the chemical charge could be reduced by synthesis, while keeping the polymer still soluble.
- Hence increasing AM (neutral and in good solvent), while keeping AMPS above 36%, does not reduce charge effects, but reduces strikingly hydrophobicity below 50% ST content.
- Styrene content, when increased above 20%, progressively dominates the hydrophobic effect, and above 50%,  $q^*$  values are close to the one of PS-co-SSNa at same ST content.
- The exponent of the scaling law between  $q^*$  and  $c_p$ ,  $\alpha$ , varies from 0.5 for hydrophilic polyelectrolytes to 0.4 for hydrophobic ones, as for partially sulfonated PSSNa.

This similarity and the smooth and consistent behaviors are in favor of both statistical copolymerization for tri-copolymers as described here, and partial sulfonated polystyrene, as used formerly.

These results will be useful to predict the behavior of other tri-co-polyelectrolytes, corresponding to the association of different repeat units, such as less hydrophobic than styrene, or charged and more hydrophobic than AMPS. Of course the Graal would be to create larger pearls, without precipitation. This would require long chains, which happens to be easier to generate with radical copolymerization.

From the synthesis point of view, this paper establishes more precisely the potential of synthesis of a large class of polyelectrolytes issued from copolymerization, for which the pearl necklace structure could be relevant, and understood. Combining different monomers can be very useful to tune solvophobicity (hydrophobicity), hence the shape of the each chain while avoiding physical association between the polymer chains.

## Acknowledgments

The Ph.D. research grant for S.BM was funded by the Tunisian Ministry of Higher Education. We warmly thank Raouf Jebali and Samir Mejdoub for their strong help in elemental

analysis of polymers at INRAP - Sidi Thabet, Mohamed Mezni and El Aiech Riahi for NMR measurements (INRAP) and Prof Hedi Mrabet from Faculté des Sciences de Tunis - Université de Tunis El Manar, for his helpful discussions.

We also warmly thank Laboratory Léon Brillouin - Saclay for beam time allocation and support, and Arnaud Helary for his strong help in the use of the PACE spectrometer at LLB. We are also grateful to Olivier Spalla from IRAMIS-CEA - Saclay for some SAXS measurements tests, to Guillaume Fleith at ICS-Strasbourg for all the SAXS measurements, and to Catherine Foussat as well as Mélanie Legros, also at ICS, for the SEC characterizations and useful discussions.

#### Appendix A. Supplementary material

Supplementary data associated with this article can be found, in the online version, at <http://dx.doi.org/10.1016/j.arabjc.2017.02.003>.

#### References

- Aseyev, V.O., Klenin, S.I., Tenhu, H., Grillo, I., Geissler, E., 2001. *Macromolecules* 34, 3706–3709.
- Aseyev, V.O., Tenhu, H., Klenin, S.I., 1998. *Macromolecules* 31, 7717–7722.
- Baigl, D., Ober, R., Dan Qu, D., Fery, A., Williams, C.E., 2003a. *Europhys. Lett.* 62, 588–594.
- Baigl, D., Seery, T.A.P., Williams, C.E., 2002. *Macromolecules* 35, 2318–2326.
- Baigl, D., Sferrazza, M., Williams, C.E., 2003b. *Europhys. Lett.* 62, 110–116.
- Barrat, J.L., Joanny, J.F., 1996. In: Prigogine, I., Rice, S.A. (Eds.), *Advances in Chemical Physics*. New York, Wiley, vol. X C IV, and references therein.
- Chepelianskii, A.D., Mohammad-Rafiee, F., Trizac, E., Raphael, E., 2009. *J. Phys. Chem. B* 113, 3743–3749.
- Combet, J., Isel, F., Rawiso, M., Boué, F., 2005. *Macromolecules* 38, 7456–7469.
- Combet, J., Rawiso, M., Rochas, C., Hoffmann, S., Boué, F., 2011. *Macromolecules* 44, 3039–3052.
- Cotton, J.P., LLB Web site, <<http://www-llb.cea.fr>> .
- Dan Qu, D., Baigl, D., Williams, C.E., Mohwald, H., Fery, A., 2003. *Macromolecules* 36, 6878–6883.
- De Gennes, P.G., Pincus, P., Velasco, R.M., Brochard, F., 1976. *J. de Phys. Paris* 37, 1461–1473.
- Di Cola, E., Plucktaveesak, N., Waigh, T.A., Colby, R.H., Tan, J.S., Pyckhout-Hintzen, W., Heenan, R.K., 2004. *Macromolecules* 37, 8457–8465.
- Dobrynin, A.V., Colby, R.H., Rubinstein, M., 1995. *Macromolecules* 28, 1859–1871.
- Dobrynin, A.V., Rubinstein, M., 1999. *Macromolecules* 32, 915–922.
- Dobrynin, A.V., Rubinstein, M., 2001. *Macromolecules* 34, 1964–1972.
- Dobrynin, A.V., Rubinstein, M., Obukhov, S.P., 1996. *Macromolecules* 29, 2974–2979.
- Dubois, E., Boué, F., 2001. *Macromolecules* 34, 3684–3697.
- Essafi, W., Raissi, W., Abdelli, A., Boué, F., 2014. *J. Phys. Chem.* 118, 12271–12281.
- Essafi, W., Haboubi, N., Williams, C.E., Boué, F., 2011. *J. Phys. Chem. B* 115, 8951–8960.
- Essafi, W., Lafuma, F., Williams, C.E., 1995. *J. Phys. II* 5, 1269–1275.
- Essafi, W., Lafuma, F., Baigl, D., Williams, C.E., 2005. *Europhys. Lett.* 71, 938–944.
- Essafi, W., Lafuma, F., Williams, C.E., Schmitz, K.S. (Eds.), 1994. *ACS Symposium Series* 548, 278–286.
- Essafi, W., Lafuma, F., Williams, C.E., 1999. *Eur. Phys. J. B* 9, 261–266.
- Essafi, W., Spiteri, M.N., Williams, C.E., Boué, F., 2009. *Macromolecules* 42, 9568–9580.
- Goerigk, G., Schweins, R., Huber, K., Ballauf, M., 2004. *Europhys. Lett.* 66, 331–337.
- <https://www.unige.ch/sciences/chiorg/jeannerat/pdf/Tables RMN.pdf>.
- Jamshidi, H., Rabiee, A., 2014. *Adv. Mater. Sci. Eng.* 2014, 1–6.
- Jannink, G., 1986. *Makromol. Chem. Macromol. Symp.* 1, 67–80.
- Liao, Q., Dobrynin, A.V., Rubinstein, M., 2006. *Macromolecules* 39, 1920–1938.
- Li, J., Hu, Y., Vlassak, J.J., Suo, Z., 2012. *Soft Matter* 8, 8121–8128.
- Limbach, H.J., Holm, C., Kremer, K., 2002. *Europhys. Lett.* 60, 566–572.
- Limbach, H.J., Holm, C., 2003. *J. Phys. Chem. B* 107, 8041–8055.
- Manning, G.S., 1969. *J. Chem. Phys.* 51, 924–933. and 934–8.
- Micka, U., Holm, C., Kremer, K., 1999. *Langmuir* 15, 4033–4044.
- Nierlich, M., Boué, F., Lapp, A., Oberthür, R., 1985. *Colloid Polym. Sci.* 263, 955–964.
- Nierlich, M., Williams, C.E., Boué, F., Cotton, J.P., Daoud, M., Farnoux, B., Jannink, G., Picot, C., Moan, M., Wolff, C., 1979. *J. Phys. (Paris)* 40, 701–704.
- Oosawa, F.M., 1971. New York, Dekker.
- Peiffer, D.G., Kim, M.W., Kaladas, J., 1988. *Polymer* 29, 717–723.
- Rayleigh, L., 1882. *Philos. Mag.* 14, 184–186.
- Read, E., Guinaudeau, A., Wilson, D.J., Cadix, A., Violleau, F., Destarac, M., 2014. *Polym. Chem.* 5, 2202–2207.
- Schweins, R., Huber, K., 2004. *Macromol. Symp.* 211, 25.
- Schweins, R., Lindner, P., Huber, K., 2003. *Macromolecules* 36, 9564–9573.
- Sen, M., Yakar, A., Güven, O., 1999. *Polymer* 40, 2969–2974.
- Spiteri, M.N., 1997. Ph.D, Orsay University, France.
- Spiteri, M.N., Williams, C.E., Boué, F., 2007. *Macromolecules* 40, 6679–6691.
- Williams, C.E., edited by Holm, C., Kekicheff, P., Podgornik, R., 2001. *NATO Science Series*, (46) Kluwer Academic Publishers. Dordrecht, 487–586.